



Swansea University  
Prifysgol Abertawe



## Cronfa - Swansea University Open Access Repository

---

This is an author produced version of a paper published in :  
*International Journal for Numerical Methods in Engineering*

Cronfa URL for this paper:

<http://cronfa.swan.ac.uk/Record/cronfa7033>

---

### Paper:

Belblidia, F. & Bulman, S. (2002). A hybrid topology optimization algorithm for static and vibrating shell structures.  
*International Journal for Numerical Methods in Engineering*, 54(6), 835-852.

<http://dx.doi.org/10.1002/nme.450>

---

This article is brought to you by Swansea University. Any person downloading material is agreeing to abide by the terms of the repository licence. Authors are personally responsible for adhering to publisher restrictions or conditions. When uploading content they are required to comply with their publisher agreement and the SHERPA RoMEO database to judge whether or not it is copyright safe to add this version of the paper to this repository.

<http://www.swansea.ac.uk/iss/researchsupport/cronfa-support/>

# A hybrid topology optimization algorithm for static and vibrating shell structures

F. Belblidia<sup>\*,†</sup> and S. Bulman

*Department of Civil Engineering, University of Wales Swansea, Swansea SA2 8PP, U.K.*

## SUMMARY

Structural designers are reconsidering traditional design procedures using structural optimization techniques. Although shape and sizing optimization techniques have facilitated a great improvement in the emergence of new optimum designs, they are still limited by the fact that a suitable topology must be assumed initially. In this paper a hybrid algorithm entitled constrained adaptive topology optimization, or CATO is introduced. The algorithm, based on an artificial material model and an adaptive updating scheme, combines ideas from the mathematically rigorous homogenization (h) methods and the intuitive evolutionary (e) methods. The algorithm is applied to shell structures under static or free vibration situations. For the static situation, the objective is to produce the stiffest structure subject to given loading conditions, boundary conditions and material properties. For the free vibration situation, the objective is to maximize or minimize a chosen frequency. In both cases, a constraint on the structural volume/mass is applied and the optimization process is achieved by redistributing the material through the shell structure. The efficiency of the proposed algorithm is illustrated through several numerical examples of shells under either static or free vibration situations. Copyright © 2002 John Wiley & Sons, Ltd.

KEY WORDS: shells; structural topology optimization; artificial material

## 1. INTRODUCTION

This work is an extension of the fundamental research conducted by the ADOPT research group at the University of Wales Swansea led, until his untimely death, by Professor Ernest Hinton. This is a tribute to him.

Topology optimization is a tool which assists the designer in the selection of suitable initial structural topologies. The aim is to redistribute material from within a so-called reference domain in an iterative and systematic manner in order to arrive at a structural topology which is in some sense optimal.

---

\*Correspondence to: F. Belblidia, Department of Civil Engineering, University of Wales Swansea, Swansea SA2 8PP, U.K.

†E-mail: F.Belblidia@swansea.ac.uk

Contract/grant sponsor: EPSRC

*Received 24 March 2000*

*Revised 12 July 2001*

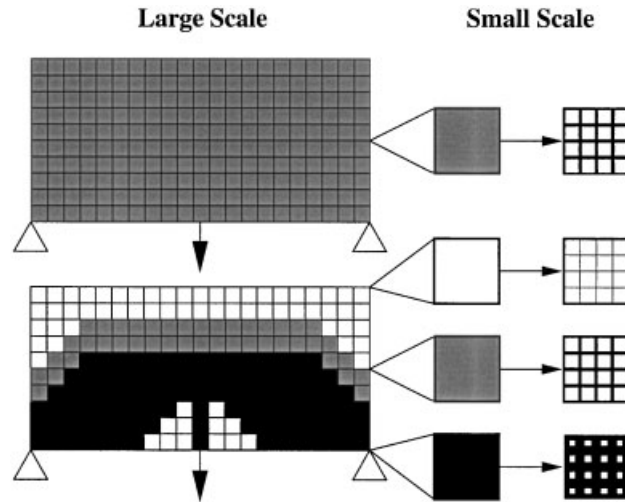


Figure 1. Basic concept of h-method topology optimization using a square microcell with a centrally placed rectangular hole as the material model: (a) top: before optimization—uniform homogenized material for all FEs; and (b) bottom: after optimization—each FE has a different material density.

There has been an extensive and continuous development in structural topology optimization techniques since the 1980s. Three major techniques have emerged, they have some common aspects such as the material format, the iterative improvement scheme and the constraint satisfaction strategy. They can be classified as follows:

- *Evolutionary methods* (e): The basic idea in the method is to use the fully stressed design techniques. In this case, inefficient material is removed from the design domain to allow the emergence of a new topology. The removal process can be achieved by either varying the elastic modulus as a function of the strain energy density as in the hard-kill/soft-kill methods [1] or by deleting from the design domain the space occupied by groups of elements with low strain energy density values as done in ESO technique [2]. This method is an intuitive engineering approach.
- *Homogenization methods* (h): The method uses the optimality criteria algorithm based on Khun–Tucker conditions. The material is represented by a sponge-like material with infinitely many micro-scale cells with voids, see Figure 1. Depending on the cell used to define the material model, we have the rank-1 and rank-2 models, the square microcell with a rectangular void [3, 4] and finally the artificial material model or SIMP method [5, 6]. The method is more mathematically based and the optimization process is achieved by the variation of the porosity of the sponge-like material throughout the structure.
- *Hybrid methods* (h/e) which contain attributes of both (e) and (h) methods in differing degrees. The first of these methods characterized the topology material in a manner similar to the microcell model of Bendsøe and Kikuchi [4] using the concept of Aboudi-cell method [7]. See Figure 2.

In the present paper, we describe the constrained adaptive topology algorithm for structural optimization, or CATO, which is an h/e-method. The algorithm uses a single layered artificial

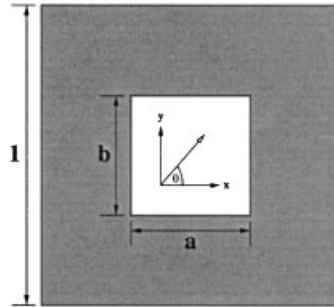


Figure 2. Bendsøe and Kikuchi classic micro-cell model: unit cell with rectangular hole in microscopic co-ordinates.

material model which consists of a porous medium. The aim of the algorithm is to find the optimum design of the structure by updating the density parameters for each element within a given design domain. The algorithm uses a mass preserving scheme which may change during the iterative improvement—hence the use of the word ‘adaptive’ in the name CATO.

The paper starts by introducing the optimization problem which can be defined as a static problem where the objective is to find the stiffest structure under a given loading and boundary conditions or a free vibration one where the objective is to optimize (maximize or minimize) a chosen natural structural frequency. A detailed description of the CATO algorithm is then introduced where the single layered artificial material model is described, followed by an explanation of the iterative material updating scheme used in the CATO algorithm. Finally, several examples are provided to demonstrate the use of the CATO algorithm in topology optimization of shell structures under either static or free vibration situations.

## 2. STRAIN ENERGY STRUCTURAL OPTIMIZATION

Many works have been undertaken for structural topology optimization based on evolutionary [1, 2] or homogenization [3–6] methods. The CATO algorithm, which is a hybrid method, has already been applied to the topology optimization of structures under plane stress/strain conditions [8].

The main purpose of the CATO algorithm is to find an optimal structural topology by using the structural material more efficiently and satisfying some basic requirements for a structural design. This is achieved by redistributing material within the structure creating zones of void (no material) and solid (material). This results in an optimum structural topology which is presented as a variable density plot. We ensure that the targeted structural mass is maintained during the complete iterative process, so that at each iteration step we have a valid solution.

For structures under static situations, the structural optimization is defined as:

Find an optimum structural topology, which corresponds to the minimum of the structural total strain energy and satisfies a structural volume/mass constraint condition. For shell structures, the total strain energy is obtained by the contribution of the membrane, bending and shear strain energy.

Therefore, the strain energy density value at each element is used as a optimization criterion in the iterative process.

### 3. NATURAL FREQUENCY STRUCTURAL OPTIMIZATION

The structural response to a dynamic loading depends, to a large extent, on the first few natural frequencies of the structure. It is often necessary to shift the fundamental or several lower frequencies of a structure away from the frequency range of a dynamic loading to avoid excessive vibrations of the structure.

A great deal of research focused on structural optimization under dynamic loading conditions has been conducted during the past three decades. Most of the work considers structural optimization with dynamic frequency constraints. The earlier work was conducted by Olhoff on optimal design of vibrating plates [9, 10], a literature survey which covers most of the work in this area can be found in Reference [11]. Recently the application of the homogenization method has been introduced with success in topology optimization of structural dynamic analysis [12–14]. Finally, the evolutionary structural optimization method [2, 15] is used to solve natural frequency optimization for vibrating structures.

The natural frequency structural optimization problem is defined as:

Find an optimum structural topology, which corresponds to the minimum or maximum of a particular natural frequency of the structure and satisfies a structural volume/mass constraint.

For the natural frequency structural optimization, let us introduce the frequency sensitivity criterion as a parameter used to perform the optimization task.

#### 3.1. Frequency sensitivity criterion

To find the best location for the material at each iteration, a factor for each element in the structure is evaluated. This sensitivity factor, which indicates the influence that the material has on the natural frequency of the structure, can be defined as follows.

The eigenvalue problem which define the dynamic behaviour of the structure is stated as

$$(\mathbf{K} - \omega_n^2 \mathbf{M})\mathbf{u}_n = 0 \quad (1)$$

where  $\mathbf{K}$  and  $\mathbf{M}$  are the global stiffness and mass matrices, respectively,  $\omega_n$  is the  $n$ th natural frequency and  $\mathbf{u}_n$  is the corresponding eigenvector. The natural frequency  $\omega_n$  and the corresponding eigenvalue  $\mathbf{u}_n$  are related to each other by the Rayleigh quotient

$$\omega_n^2 = \frac{k_n}{m_n} \quad (2)$$

in which the modal stiffness  $k_n$  and the modal mass  $m_n$  are defined as

$$k_n = \mathbf{u}_n^T \mathbf{K} \mathbf{u}_n$$

and

$$m_n = \mathbf{u}_n^T \mathbf{M} \mathbf{u}_n \quad (3)$$

The change in the frequency by the redistribution of material in the structure can be obtained by the sensitivity calculation of the frequency as

$$\Delta(\omega_n^2) = \frac{1}{m_n} (\Delta k_n - \omega_n^2 \Delta m_n) \quad (4)$$

If the material in an element  $e$  has been updated in the structure during the material redistribution scheme by creating an elemental void, the frequency sensitivity can be evaluated approximately by assuming that the eigenvector  $\mathbf{u}_n$  has not been affected by this update in the material of that particular element [11, 15], therefore

$$\begin{aligned} \Delta k_n &= \mathbf{u}_n^{(e)T} \Delta \mathbf{K} \mathbf{u}_n^{(e)} = -\mathbf{u}_n^{(e)T} \mathbf{K}^{(e)} \mathbf{u}_n^{(e)} \\ \Delta m_n &= \mathbf{u}_n^{(e)T} \Delta \mathbf{M} \mathbf{u}_n^{(e)} = -\mathbf{u}_n^{(e)T} \mathbf{M}^{(e)} \mathbf{u}_n^{(e)} \end{aligned} \quad (5)$$

in which  $\mathbf{K}^{(e)}$  and  $\mathbf{M}^{(e)}$  are the stiffness and mass matrices of the element  $e$ , and  $\mathbf{u}^{(e)}$  is the eigenvector of that element. The sensitivity of the frequency due to the update in the material of the  $e$ th element is obtain by substituting (5) into (4), so that

$$\Delta(\omega_n^2) = f^e = \frac{1}{m_n} \mathbf{u}_n^{(e)T} (\omega_n^2 \mathbf{M}^{(e)} - \mathbf{K}^{(e)}) \mathbf{u}_n^{(e)} \quad (6)$$

The sensitivity factor  $f^e$  is an indicator of the change in the natural frequency as a result of the change of the material amount in the element  $e$ . This factor is used as a criterion in the updating scheme used in CATO.

Note that expression (6) of this factor can be simplified by omitting the modal mass  $m_n$  from (6) as  $m_n$  is the same for every element in the structure. Note that the summation of the sensitivity factor over all the elements is equal to zero which is useful for checking the correctness of the code [2].

Note that in the present work we are involved in the minimization (or the maximization) of a particular frequency without taking into account the effect of cross-over of modes: as, for example, the first frequency is increasing, the second frequency is decreasing and it can happen that the two frequencies meet. To avoid the cross-over phenomenon we can, in this case, while minimizing (or maximizing) a particular frequency, keep the difference between it and its closest frequency constant. This can be done by adding a constraint to the optimization problem. This idea has not been implemented in the present work.

#### 4. CONSTRAINED ADAPTIVE TOPOLOGY OPTIMIZATION ALGORITHM

Let us describe the main features of the CATO algorithm. Firstly, the single layered artificial material model is introduced, followed by a detailed explanation of the iterative material updating scheme process. Finally, several examples are presented to show the performance of the proposed algorithm for shell structures under static and free vibration situations.

#### 4.1. Artificial material model

By considering structural topology optimization as a material distribution problem, the structure can be described by a discrete function  $\chi$ , defined at each point  $\mathbf{x}$  as

$$\chi(\mathbf{x}) = \begin{cases} 1 & \text{if } \mathbf{x} \in \Omega_s \quad \text{material,} \\ 0 & \text{if } \mathbf{x} \in \Omega \setminus \Omega_s \quad \text{no material} \end{cases} \quad (7)$$

where  $\Omega$  is the design domain,  $\Omega_s$  is the solid part of it and  $\mathbf{x} \in \Omega$  is the vector of design variables.

If isotropic behaviour is assumed for the solid part of the structure, we can write

$$\rho(\mathbf{x}) = \chi(\mathbf{x})\rho^0 \quad \text{and} \quad \mathbf{D}(\mathbf{x}) = \chi(\mathbf{x})\mathbf{D}^0 \quad (8)$$

where  $\rho^0$  and  $\mathbf{D}^0$  are the density and elastic constitutive matrix, respectively, of the homogeneous solid. Note that  $\rho(\mathbf{x})$  is related to the mass matrix  $\mathbf{M}$  and  $\mathbf{D}(\mathbf{x})$  is also related to the stiffness matrix  $\mathbf{K}$ .

For the numerical solution of the optimization problem, the discrete function  $\chi$  causes solution difficulties [4]. One easy way to overcome these difficulties is to replace the discrete function  $\chi$  by a continuous one  $\xi$ , where  $0 \leq \xi(x) \leq 1$ . As a convenient fiction we will assume that the material has a micro-cellular structure and each cell is a square with a square hole of side length  $a$  where  $0 \leq a \leq 1$ . Thus, in the present model

$$\xi(x) = 1 - a^2(x) \quad (9)$$

Note that by changing the size of the void, which is used as a design variable, we are able to create a micro-cellular void ( $a=1$ ) or solid ( $a=0$ ). CATO uses this concept to redistribute material iteratively in the structure.

It is desirable to obtain a solution which only consists of solid and void regions. This allows a better approximation to condition (7). Rozvany [5] suggested that porous regions could be suppressed by adding to the material costs the 'cost of manufacturing of holes', thereby a parameter  $\mu$  can be included to penalize the intermediate values of  $\xi(\mathbf{x})$ . Hence

$$\rho(\mathbf{x}) = \xi(\mathbf{x})^\mu \rho^0 \quad \text{and} \quad \mathbf{D}(\mathbf{x}) = \xi(\mathbf{x})^\mu \mathbf{D}^0 \quad (10)$$

where the exponent  $\mu > 1$  and is usually between 3 and 9.

Note that although we have assumed a micro-cellular material with square hole size  $a$ , we have approximated the resulting material behaviour as though it were isotropic based on solid isotropic microstructure with penalty (SIMP [5, 6]) method rather than truly orthotropic. There is, therefore, no dependency on the orientation of the square hole in the artificial material model unlike the case for the more conventional micro-cell model.

#### 4.2. The CATO algorithm

For structure under static situation, the elemental strain energy density values  $f^e$  are obtained from a static analysis at each iteration. These values are ordered in an ascending manner.

For free vibration optimization problem, the result of the sensitivity factor values  $f^e$  for each element are obtained from a free vibration analysis at each iteration for a chosen frequency, CATO orders these values according to the type of frequency optimization required

- in a ascending order of  $f^e$  for a frequency minimization problem, or
- in a ascending order of  $-f^e$  for a frequency maximization problem. This allows the use of the same algorithm for both natural frequency minimization or maximization problem.

The CATO algorithm is now summarized in the following steps. Note that we have used the standard term ‘design’ and ‘non-design’ domain to refer to zones in which the density parameters are allowed to change and zones where they are not.

1. Define the optimization problem type (static or free vibration). Set up the design domain data, optimization data and FE model data including information defining the mesh, material properties, boundary conditions and loading conditions for the static case. Set iteration counter  $i = 1$ .
2. For the desired mass fraction,  $M_{\text{fac}}$ , initialize the material density parameters  $a_i^e$  for each element according to the expressions

$$a_i^e = \begin{cases} 0 & \text{if non-design domain} \\ (1 - M_{\text{fac}})^{1/2} & \text{if design} \\ a_{\text{pr}} & \text{if prescribed} \end{cases}$$

Calculate the desired mass of the system  $M_{\text{des}}$  using

$$M_{\text{des}} = M_{\text{fac}} * \sum_{e=1}^n \rho^e v^e$$

where  $n$  is the number of elements in the design domain and  $\rho^e$  and  $v^e$  are the density and the volume of element  $e$ , respectively.

3. For the current  $a_i^e$  values evaluate the appropriate constitutive properties using an artificial material model. See Section 4.1.
4. Depending on the optimization problem, perform a static or a free vibration analysis.
5. Order the elements according to their values  $f^e$ .
6. From a specified mass preserving relationship  $\Delta a_i^e(f^e)$  evaluate the change of the density parameters  $\Delta a_i^e$  for each element and update the density parameter so that  $a_{i+1}^e = a_i^e + \Delta a_i^e$ . See Section 4.3.
7. Given the new density parameters  $a_{i+1}^e$ , evaluate the overall structural mass of the system  $M_{\text{sys}}$ .
8. Check the requirement that  $M_{\text{sys}}/M_{\text{des}} < M_{\text{tol}}$ . If this condition is not satisfied, adjust  $a_{i+1}^e$  proportionately to obtain  $M_{\text{sys}} = M_{\text{des}}$  and go to step 7.
9. If some convergence criterion is met continue to step 10, otherwise set  $i = i + 1$  and return to step 3.
10. Post-process the results prior to visualization and then terminate the solution.

#### 4.3. Material updating scheme for structural optimization

The CATO algorithm uses an incremental relationship  $\Delta a^e(f^e)$  to adjust the elemental material parameter  $a^e$  according to the element factor value  $f^e$  related to the optimization problem type. A special feature of this relationship is that it is chosen so as to preserve the total mass of the structure during the optimization iterative process. Figure 3 shows an example of this



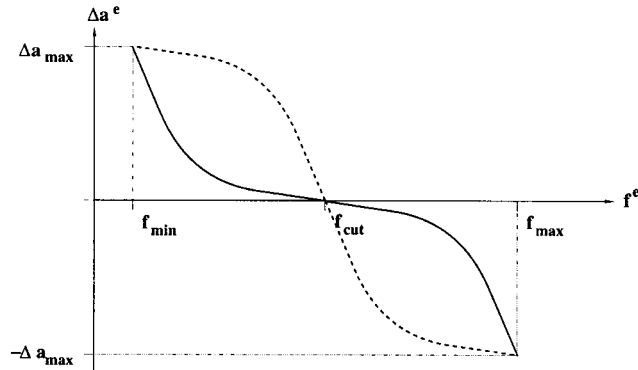


Figure 3. Example of the relationship  $\Delta a^e(f^e)$  at an early stage of the iterative scheme (solid line), and at an intermediate stage (dash line).

relationship at two stages of the scheme. The function is composed of a curve of the form  $y = n^{p_{\text{cur}}}$  ( $n$  and  $p_{\text{cur}}$  are described later).

To define the curve some parameters are needed. If  $\ell = [\ell^1, \ell^2, \dots, \ell^n]^T$  is the list of  $n$  element numbers ordered with regard to the type of optimization problem, then three parameter values  $f_{\text{min}}$ ,  $f_{\text{max}}$  and  $f_{\text{cut}}$  are calculated as

$$\begin{aligned} f_{\text{min}} &= f^{(\ell^1)} \\ f_{\text{max}} &= f^{(\ell^n)} \end{aligned} \quad (11)$$

and

$$f_{\text{cut}} = f^{(\ell^k)}$$

where  $k$  satisfies the equation

$$\sum_{i=k}^n \rho^{\ell^i} v^{\ell^i} = M_{\text{des}} \quad (12)$$

and  $\rho^{\ell^i}$  and  $v^{\ell^i}$  are the density and volume of element  $\ell^i$ , respectively.

The change in the density parameter  $\Delta a_i^e$  for element  $e$  at iteration  $i$  is illustrated in Figure 3 and is given by

$$\Delta a_i^e = \alpha n^{p_{\text{cur}}} \quad (13)$$

where

$$\begin{aligned} \alpha &= -\frac{f^e - f_{\text{cut}}}{|f^e - f_{\text{cut}}|} \\ n &= \frac{f^e - f_{\text{cut}}}{r} \end{aligned} \quad (14)$$

$$p_{\text{cur}} = p_{\text{init}} - (i - 1.0) \times \text{iter}$$

and  $r$  is defined as

$$r = \begin{cases} f_{\max} - f_{\text{cut}} & \text{if } f^e > f_{\text{cut}} \\ f_{\min} - f_{\text{cut}} & \text{if } f^e \leq f_{\text{cut}} \end{cases} \quad (15)$$

Three further parameters are specified by the user, they are: (a) The maximum incremental density parameter  $\Delta a_{\max}$  which governs the maximum allowable change in  $\Delta a^e$  at any one iteration cycle. (b) The initial curve exponent parameter  $p_{\text{init}}$  determines the initial configuration of the curve. Finally, (c) The iterative advancing parameter  $iter$  controls how the curve adapts through the iterative scheme.

Once the density parameters  $a_i^e$  for all elements in the design domain have been updated the mass of the new system is evaluated to check that the mass fraction constraint is not violated using the expression

$$|M_{\text{sys}}/M_{\text{des}}| < M_{\text{tol}} \quad (16)$$

where  $M_{\text{sys}}$  is the current structural mass of the system,  $M_{\text{des}}$  is the desired mass and  $M_{\text{tol}}$  is some allowable tolerance on the mass constraint.

If (16) is satisfied, then the algorithm can proceed to the next iteration. However, if (16) is not satisfied then the mass error for each element is calculated as

$$M_{\text{err}} = \frac{M_{\text{sys}} - M_{\text{des}}}{n} \quad (17)$$

where  $n$  is the number of elements in the design domain. The new density parameter  $a_{i+1}^e$  for each element is then simply taken as

$$a_{i+1}^e = a_i^e + M_{\text{err}} \quad (18)$$

#### 4.4. Convergence

Two termination criteria are used in CATO process, if one of them is satisfied, the topology optimization is terminated. These criteria are:

1. the number of iterations exceeds a number specified by the user, or
2. the change in the objective function (strain energy, or frequency) at any two successive iterations is below a given tolerance.

After convergence some post-processing of the results is conducted which included a thresholding technique in order to get a black and white topology image.

## 5. EXAMPLES

CATO is now illustrated for several problems involving shell structures under static situations in Section 5.1 and free vibration situations in Section 5.2.

For all examples, a single layered artificial material is considered and the common parameters used for the CATO algorithm in all examples are: maximum incremental density parameter  $\Delta a_{\max} = 0.05$ , the initial curve exponent parameter  $p_{\text{init}} = 5.0$ , and the iterative advancing parameter  $iter$  is 0.05. A maximum of 100 iterations is assumed with a convergence

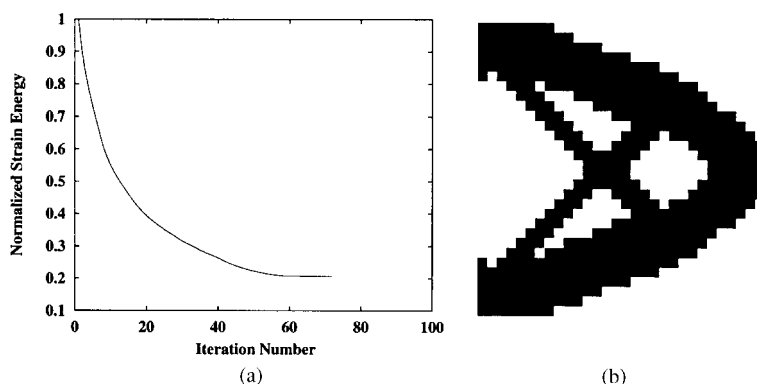


Figure 4. Clamped square plate under a point load: (a) convergence of the normalized strain energy; and (b) optimal stiffening topology.

tolerance in the change of the objective function of 1%. For each example, the convergence history is given with the optimum topology design as a black and white image. All units are assumed to be consistent.

We should note that because we are using the artificial material model, the density values (strain energy or natural frequency) obtained during the iterative process are normalized by their maximum value.

### 5.1. Shell structures under static situation

**5.1.1. Square plate under plane stress behaviour.** A square plate clamped on the left-hand edge and subjected to a point load applied at middle of the free edge opposite the clamped edge.

The problem data is: elastic modulus  $E=2.1 \times 10^5$ , Poisson's ratio  $\nu=0.3$ , and load magnitude  $F=100$ . A structured FE mesh consisting of 900 ( $30 \times 30$ ) quadrilateral nine-noded shell elements is used to represent the plate. The plate side length is  $a=10$ , and the thickness is  $h=0.1$ . A mass fraction of 50% is considered.

Figure 4(a) illustrates the variation of the normalized strain energy with increasing number of iterations while Figure 4(b) shows the optimal stiffening topology at 72 iterations. There is a decrease in the strain energy of about 80%.

**5.1.2. Clamped square plate under bending behaviour.** We now consider a clamped supported square plate under central point load, the problem data is: elastic modulus  $E=10.92 \times 10^5$ , Poisson's ratio  $\nu=0.3$ , load magnitude  $F=100$ . A structured FE mesh consisting of 625 ( $25 \times 25$ ) quadrilateral nine noded shell elements is used to idealize the plate quadrant. The plate side length is  $a=10$  and the thickness is  $h=0.1$ . A mass fraction of 50% is considered.

In this example only a symmetric quadrant of the plate is analysed, however, the topology image shows the result for the whole plate.

Figure 5(a) illustrates the variation of the normalized strain energy with increasing number of iterations while Figure 5(b) shows the optimal stiffening topology at 69 iterations. There is a decrease in the strain energy of about 85%.

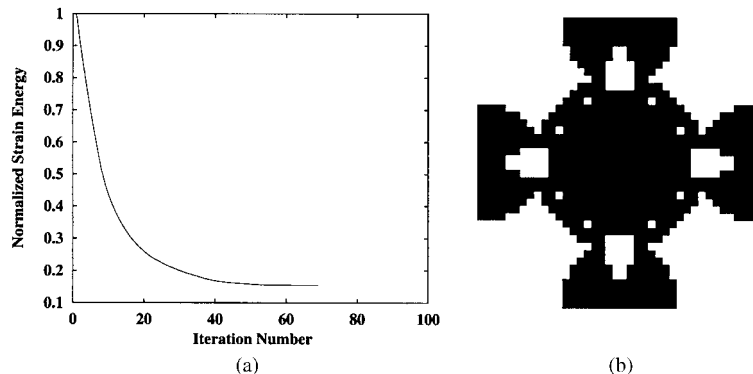


Figure 5. Clamped supported square plates under central point load: (a) convergence of the normalized strain energy; and (b) optimal stiffening topology.

*5.1.3. Elliptic paraboloid (EP) shell with parabolic edges.* The EP shell surface is obtained by translating a hogging parabola over another hogging parabola fixed in a vertical plane, while keeping the plane of the moving parabola vertical and at right angles to the plane of the fixed parabola. The surface equation can be expressed by

$$z(x, y) = \frac{k}{a^2} (x^2 + y^2)$$

where  $k$  is equal to 0.13. The shell has a centrally applied point load and its four edges are clamped. Only the symmetric quadrant is considered.

A structured FE mesh consisting of 400 ( $20 \times 20$ ) quadrilateral nine noded shell elements is used to idealize the symmetric quadrant and its projection on the  $xy$  plane is a square of side length  $a=100$ .

The problem data is: elastic modulus  $E=10.92 \times 10^3$ , Poisson's ratio  $\nu=0.3$ , load magnitude  $F=100$ , and the shell thickness  $h=0.01$ . A mass fraction of 50% is considered.

Figure 6(a) shows the variation of the normalized strain energy with increasing number of iterations for the EP shell. The optimal topology is shown in Figure 6(b) at 55 iterations. We notice a decrease in the strain energy of about 80%.

*5.1.4. Conoid shell.* In this example, the shell has three straight edges and a curved edge defined by the conoid parabolic surface

$$z(x, y) = \frac{ky}{a} \times \left( 1 - \frac{y^2}{a^2} \right)$$

where the curvature factor  $k$  is taken equal to 50.0. The curved edge is aligned with the  $x$ -axis and the shell geometry is interpolated linearly along the  $y$ -axis. Both ends of the curved edge are supported by a hinge and the straight edge opposite to the curved edge is clamped. The other edges are free. The shell is subjected to a centrally applied point load. A structured FE mesh consisting of 400 ( $20 \times 20$ ) quadrilateral nine noded shell elements is used to idealize the symmetric half of the shell. The projection of the shell half on the  $xy$  plane is a square of side length  $a=100$ . The problem data used for the EP shell is again used here.

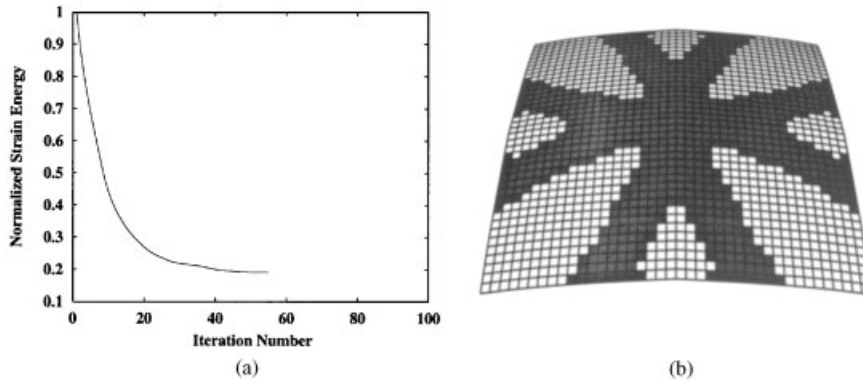


Figure 6. Clamped at four edges EP shell subjected to a centrally applied point load: (a) convergence of the normalized strain energy; and (b) optimal stiffening topology.

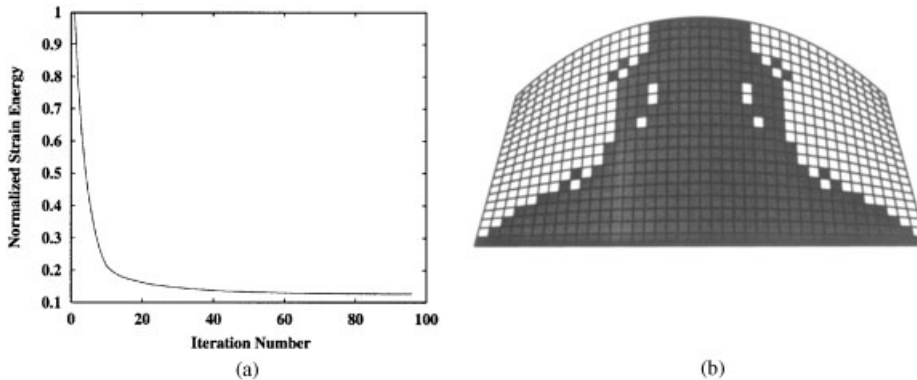


Figure 7. Conoid shell subjected to a centrally applied point load: (a) convergence of the normalized strain energy; and (b) optimal stiffening topology.

Figure 7(a) shows the variation of the normalized strain energy with increasing number of iterations for the conoid shell while Figure 7(b) shows the optimal topology for this shell at 96 iterations. There is a decrease in the strain energy of about 88%.

### 5.2. Shell structures under free vibration situation

Note that when dealing with a frequency minimization, it can happen that the structure connectivity collapses leading to a non-defined structure with a minimum null frequency due to the use of a single layered material model. In this case, the user can stop the iterative process or a structural connectivity criterion can be introduced [16]. In CATO when dealing with a minimization problem, no thresholding is used and therefore the final topology result is a grey scaled image. Note also that in the present study there is no control on the cross-over modes phenomenon.

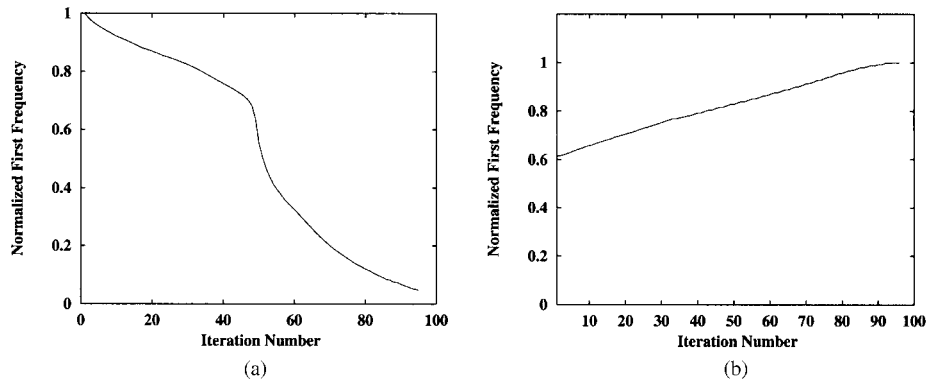


Figure 8. Convergence of normalized frequency of a square 2D plate example: (a) minimize the first frequency; and (b) maximize the first frequency.

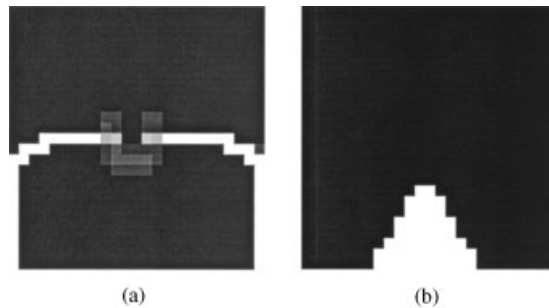


Figure 9. Topology optimization results of a square 2D plate example: (a) minimize the first frequency; and (b) maximize the first frequency.

*5.2.1. Square plate under plane stress behaviour.* A square plate of dimension  $10 \times 10$  is clamped at three sides as in Reference [2]. The whole plate is meshed with  $25 \times 25$  nine-noded elements. The problem data are: elastic modulus  $E = 70000.0$ , Poisson's ratio  $\nu = 0.3$ , mass density  $\rho = 2700$ , and the plate thickness  $h = 0.01$ . Two topology optimization problems are investigated dealing with (a) the minimization and (b) the maximization of the first frequency using a mass fraction of  $M_f = 92\%$  and a penalty exponent for the artificial material of  $\mu = 3$ .

Figure 8 illustrates the variation of the normalized first frequency for cases (a) and (b), respectively, while Figure 9 shows their respective optimal stiffening topologies. The topology results are in good agreement with Xie and Steven [2].

*5.2.2. Clamped square plate under bending behaviour.* The plate introduced earlier in Section 5.1.2 is used for natural frequency optimization using the following data: elastic modulus  $E = 70000.0$ , Poisson's ratio  $\nu = 0.3$ , mass density  $\rho = 2700$ , and the plate thickness  $h = 0.01$ .

The optimization problems are defined as (a) minimizing the first frequency or (b) maximizing it using a mass fraction of  $75\%$  and a penalty exponent of  $\mu = 5$ .

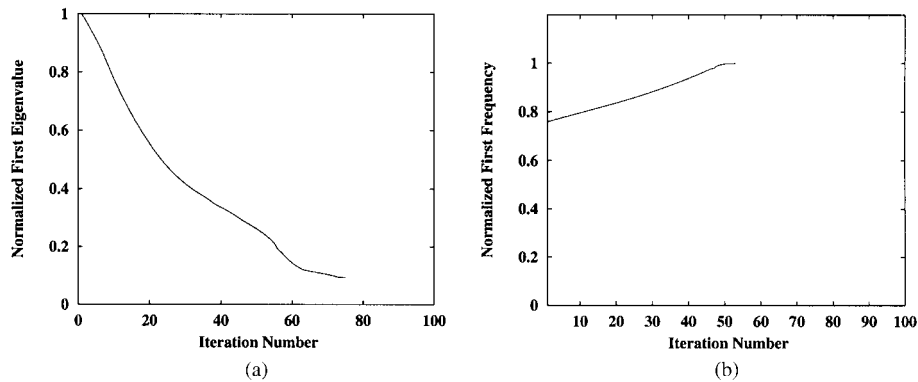


Figure 10. Convergence of normalized frequency of a clamped square plate example: (a) minimize the first frequency; and (b) maximize the first frequency.

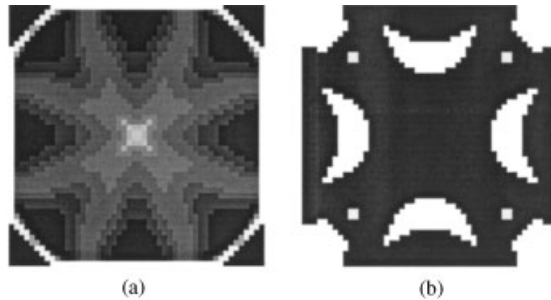


Figure 11. Topology optimization results of a clamped square plate example: (a) minimize the first frequency; and (b) maximize the first frequency.

Figure 10 illustrates the variation of the normalized first frequency for cases (a) and (b), respectively. Note that there is a decrease about 90% after 78 iterations in case (a) and an increase about 25% after 53 iterations in case (b). Figure 11 shows their respective optimal stiffening topologies for the whole plate. Note that topology image for case (a) is, to some extent, similar to the ‘negative’ image of case (b).

**5.2.3. Elliptic paraboloid (EP) shell with parabolic edges.** The EP shell described in Section 5.1.3 is again investigated here using the same geometry, mesh and the following problem data: elastic modulus  $E=70000.0$ , Poisson’s ratio  $\nu=0.3$ , mass density  $\rho=2700$ , and the plate thickness  $h=0.01$ .

The optimization problems are defined as (a) minimizing the first frequency, (b) maximizing it, or (c) maximizing the second frequency using a mass fraction of 75% and a penalty exponent of  $\mu=5$ .

Figure 12 illustrates the variation of the normalized frequency for (a) minimized the first frequency, (b) maximized the first frequency and (c) maximized the second frequency, respectively, while Figure 13 shows their respective optimal stiffening topologies for the whole shell. Note that after 29 iterations there is a clear collapse of the shell in case (a) while after

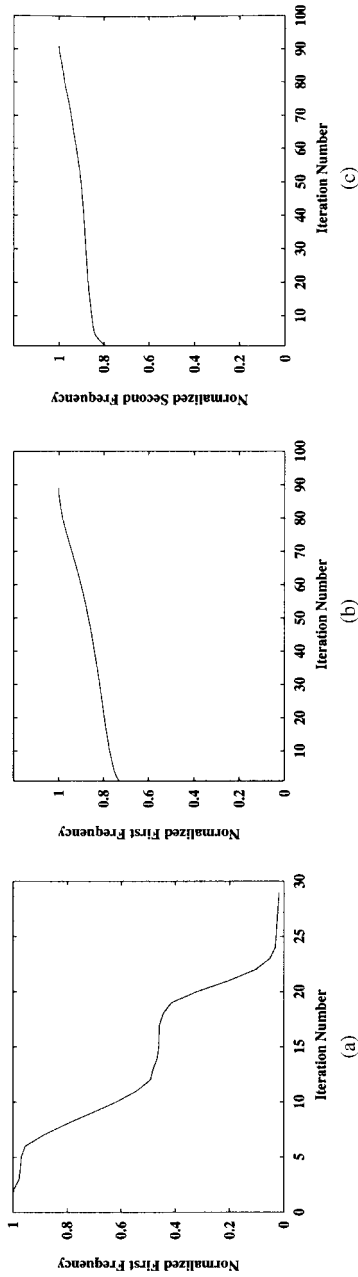


Figure 12. Convergence of normalized frequency of a clamped EP shell example: (a) minimize the first frequency; (b) maximize the first frequency; and (c) maximize the second frequency.

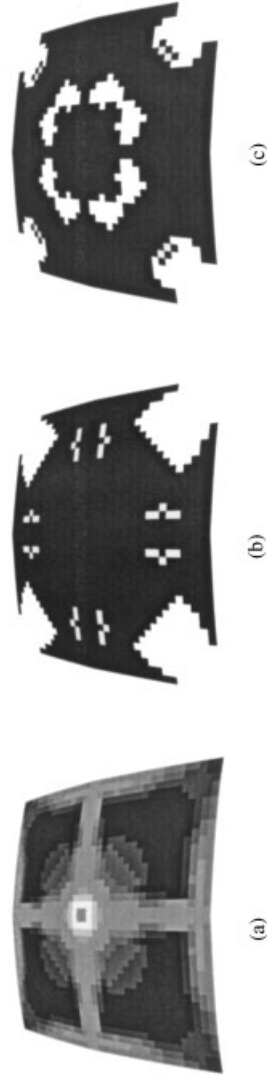


Figure 13. Topology optimization results of a clamped EP shell example; (a) minimize the first frequency; (b) maximize the first frequency; and (c) maximize the second frequency.



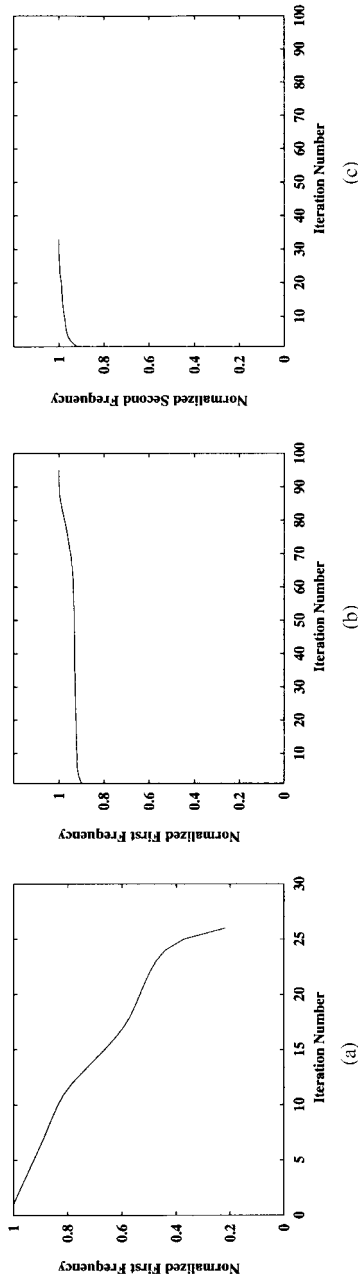


Figure 14. Convergence of normalized frequency of a conoid shell example: (a) minimize the first frequency; (b) maximize the first frequency; and (c) maximize the second frequency.



Figure 15. Topology optimization results of a conoid shell example: (a) minimize the first frequency; (b) maximize the first frequency; and (c) maximize the second frequency.

89 iterations and 92 iterations there is an increase about 25 and 20% in cases (b) and (c), respectively.

5.2.4. *Conoid shell.* The conoid shell introduced before (Section 5.1.4) is considered for natural frequency optimization based on the same data as the EP shell (Section 5.2.3).

Figure 14 illustrates the variation of the normalized frequency for (a) minimized the first frequency, (b) maximized the first frequency and (c) maximized the second frequency, respectively, while Figure 15 shows their respective optimal stiffening topologies for the whole shell. Here in case (a) the convergence is reached in 26 iteration with a decrease about 80% in the first frequency minimization and a small increase about 10 and 7% for the first and second frequency maximization respectively.

## 6. CONCLUSIONS

This paper has illustrated the use of the CATO algorithm for topology optimization of shell structures under static and free vibration situations. The algorithm combines ideas from both conventional (h) and (e) methods. Several examples are introduced and can be compared with previously known work with favorable results. The convergence to the optimum shell design is reached in < 100 iterations in both cases.

In static case, for the examples introduced here there have been a decrease in the strain energy of 80–88%. For the natural frequency minimization problem no thresholding has been used avoid the collapse of structural connectivities. We have noticed that for a minimization of a particular frequency, the topology image is quite similar to the ‘negative’ of the image of the maximization of that particular frequency.

## ACKNOWLEDGEMENT

The authors gratefully acknowledge the sponsorship provided by the EPSRC for the FIDO project.

## REFERENCES

1. Hinton E, Sienz J. Fully stressed topological design of structures using an evolutionary procedure. *Engineering Computational* 1995; **12**:229–244.
2. Xie YM, Steven GP. *Evolutionary Structural Optimization*. Springer: Berlin, 1997.
3. Bendsøe MP. *Optimization of Structural Topology Shape, and Material*. Springer: Berlin, 1995.
4. Bendsøe MP, Kikuchi N. Generating optimal topologies in structural design using homogenization method. *Computer Methods in Applied Mechanics and Engineering* 1988; **71**:197–224.
5. Zhou M, Rozvany GIN. The COC algorithm, Part II: Topological, geometrical and generalized shape optimization. *Computer Methods in Applied Mechanics and Engineering* 1991; **89**:309–336.
6. Rozvany GIN, Zhou M, Birker T. Generalized shape optimization without homogenization. *Structural Optimization* 1992; **4**:250–252.
7. Paley M, Fuchs MB, Miroshnik E. The Aboudi micromechanical model for shape design of structures. *Proceedings of the Third International Conference on Computational Structures Technology*, Budapest, August, 1996.
8. Bulman S, Hinton E. Constrained adaptive topology optimization of engineering structures. *Design Optimization* 1999; **1**:419–439.
9. Olhoff N. Optimal design of vibrating circular plates. *International Journal of Solids and Structures* 1970; **6**:139–156.
10. Olhoff N. Optimal design of vibrating rectangular plates. *International Journal of Solids and Structures* 1974; **10**:93–109.

11. Grandhi RV. Structural optimization with frequency constraints—a review. *AIAA Journal* 1993; **31**:2296–2303.
12. Díaz AR, Kikuchi N. Solution to shape and topology eigenvalue optimization problems using a homogenization method. *International Journal for Numerical Methods in Engineering* 1992; **35**:1487–1502.
13. Ma ZD, Kikuchi N, Cheng HC, Hagiwara I. Topology and shape optimization methods for structural dynamic problems. In: Pedersen P (ed.). *Optimal Design with Advanced Materials*. Elsevier: Oxford, 1993; 247–261.
14. Tenek LH, Hagiwara I. Static and vibrational shape and topology optimization using homogenization and mathematical programming. *Computer Methods in Applied Mechanics and Engineering* 1993; **109**:143–154.
15. Xie YM, Steven GP. Evolutionary structural optimization for dynamic problems. *Computers and Structures* 1996; **58**:1067–1073.
16. Zhao C, Steven GP. Evolutionary natural frequency optimization of thin plate bending vibration problem. *Structural Optimization* 1996; **11**:244–251.